Electronic Supplementary Material (ESI) for Materials Advances.
This journal is © The Royal Society of Chemistry 2020

Electronic Supplementary Information (ESI)

Urchin-like NiCoP coated with carbon layer as high performance electrodes for all-solid-state asymmetric supercapacitors

Jingzhou Ling[a], Hanbo Zou[a,*], Wei Yang[b], Shengzhou Chen[b,**]

a. School of Chemistry and Chemical Engineering, Guangzhou University, Guangzhou, China

b. Guangzhou Key Laboratory for New Energy and Green Catalysis, Guangzhou University, Guangzhou, China

[*] Corresponding author. Tel: +86 20 39366906; Fax: +86 20 39366902.
[**] Corresponding author. Tel: +86 20 39339685; Fax: +86 20 39339685.
E-mail address: zouhb@gzhu.edu.cn (H. B. Zou)
szchen@gzhu.edu.cn (S. Z. Chen)

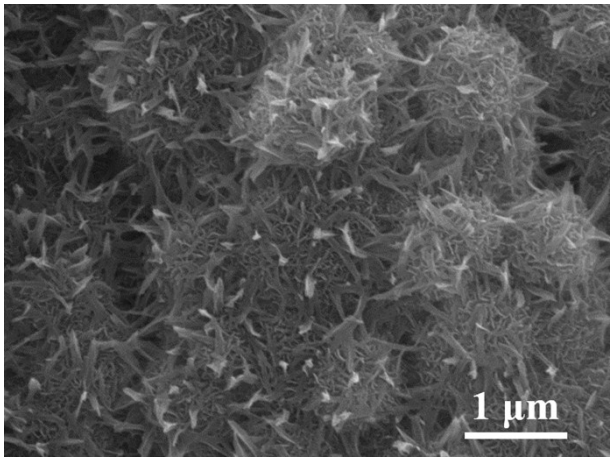

Fig. S1. High magnification SEM image of NiCo-ULAs precursor obtained from hydrothermal reaction for 2 h.

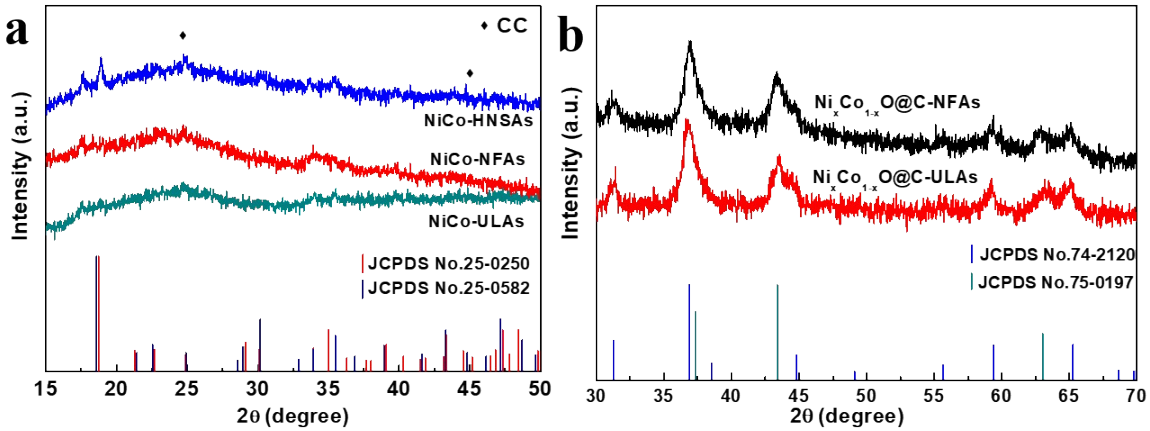

Fig. S2. (a) XRD patterns of as-prepared NiCo-NFAs, NiCo-ULAs and NiCo-HNSAs. The diffraction peaks of the three XRD patterns can be indexed to $CoC_2O_4 \cdot 2H_2O$. (b) XRD patterns of $Ni_xCo_{1-x}O$@C-NFAs and $Ni_xCo_{1-x}O$@C-ULAs.

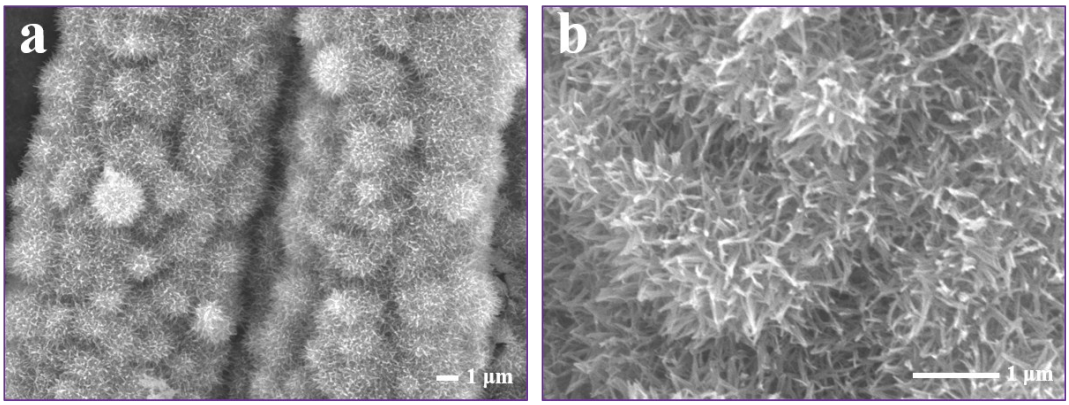

Fig. S3. (a) Low and (b) high magnification SEM images of $Ni_xCo_{1-x}O$@C-ULAs.

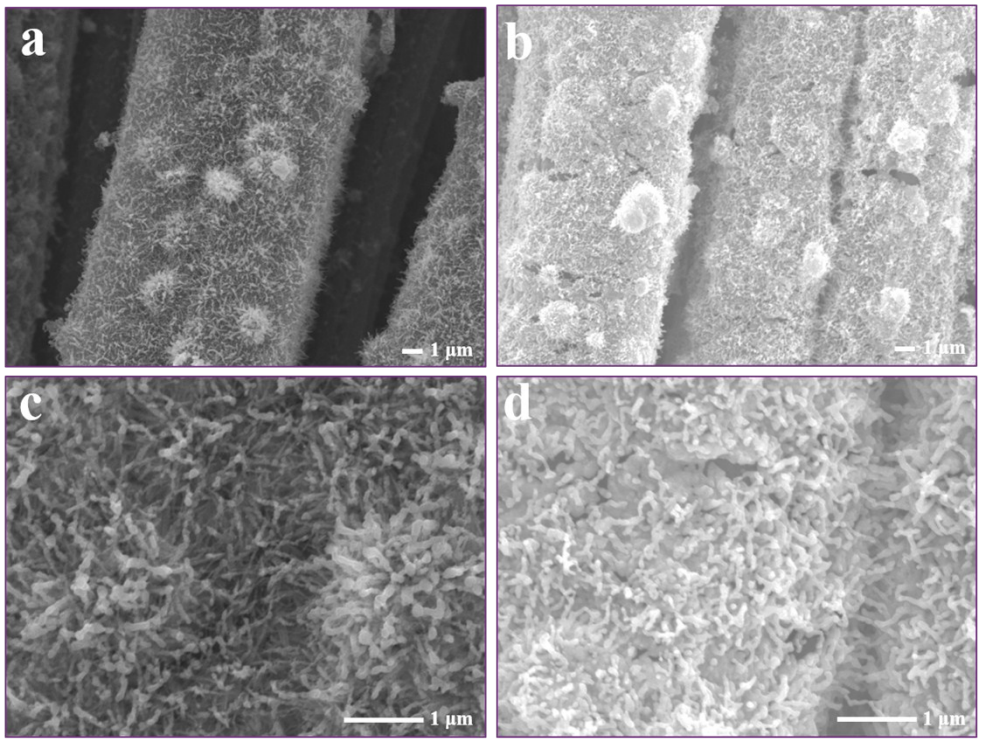

Fig. S4. SEM images of the hybrids (phosphides coated with carbon) obtained with the various glucose concentration of (a, c) 0.03 M and (b, d) 0.04 M.

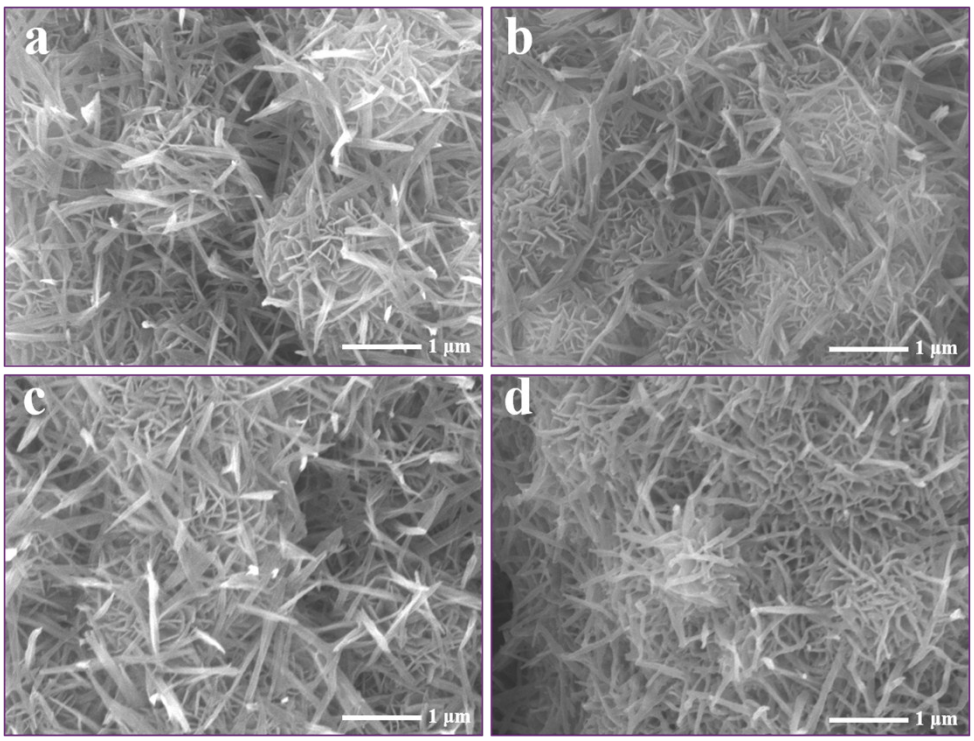

Fig. S5. SEM images of (a) NiCo-NFAs, (b) NiCoP-NFAs, (c) $Ni_xCo_{1-x}O$@C-NFAs, and (d) NiCoP@C-NFAs.

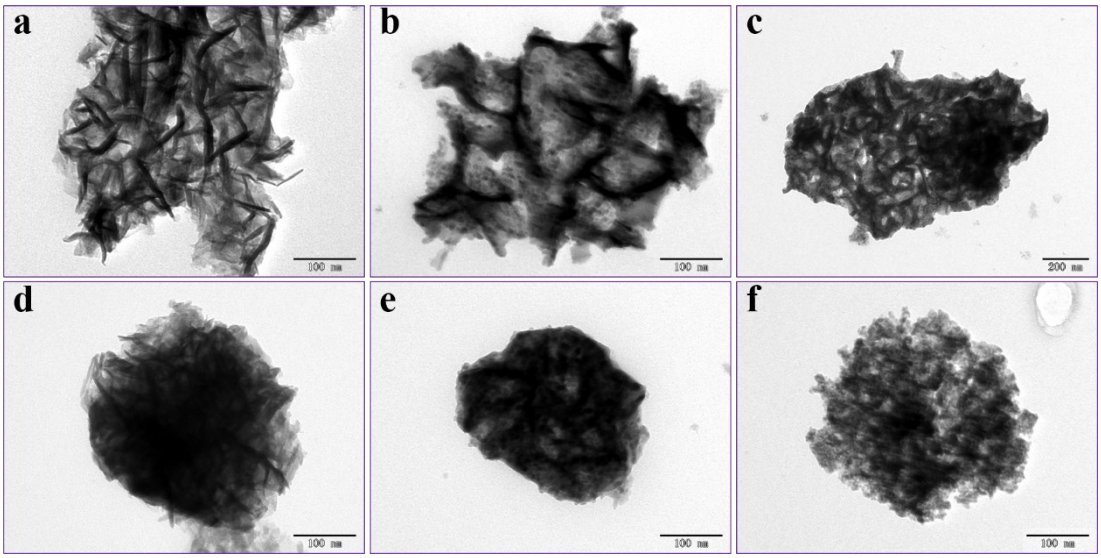

Fig. S6. TEM images of (a) NiCo-NFAs, (b) NiCoP-NFAs, (c) NiCoP@C-NFAs, (d) NiCo-ULAs, (e) NiCoP-ULAs, and (f) NiCoP@C-ULAs.

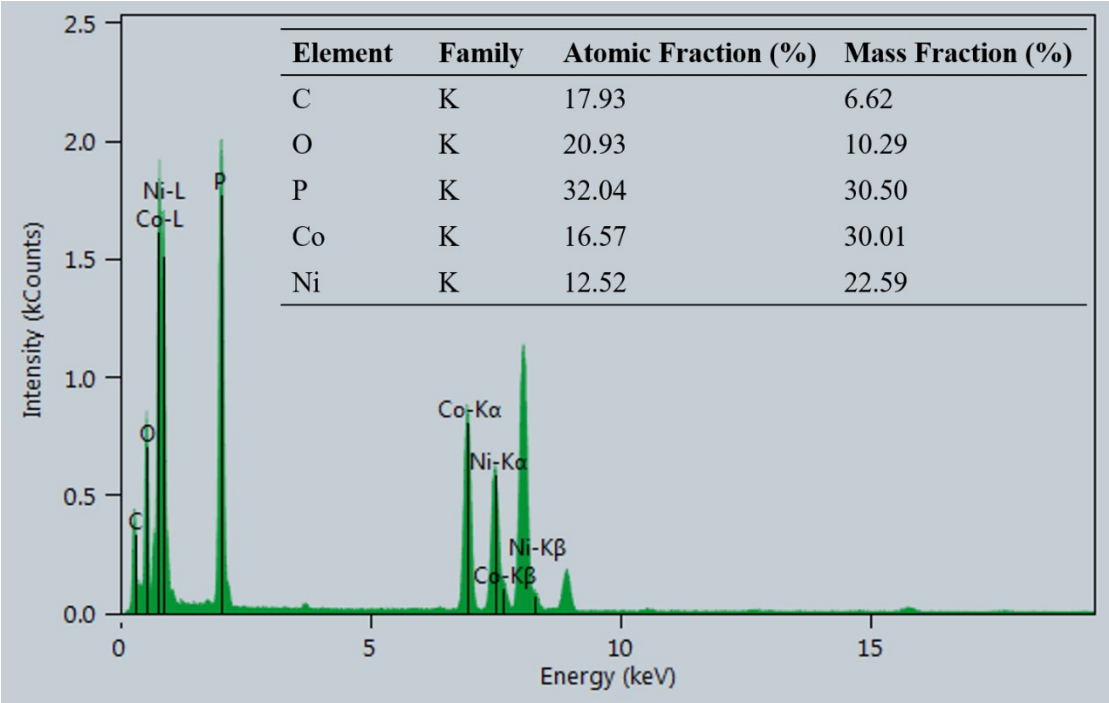

Element	Family	Atomic Fraction (%)	Mass Fraction (%)
C	K	17.93	6.62
O	K	20.93	10.29
P	K	32.04	30.50
Co	K	16.57	30.01
Ni	K	12.52	22.59

Fig. S7. EDX spectrum of NiCoP@C-ULAs, and the inset of corresponding the element content.

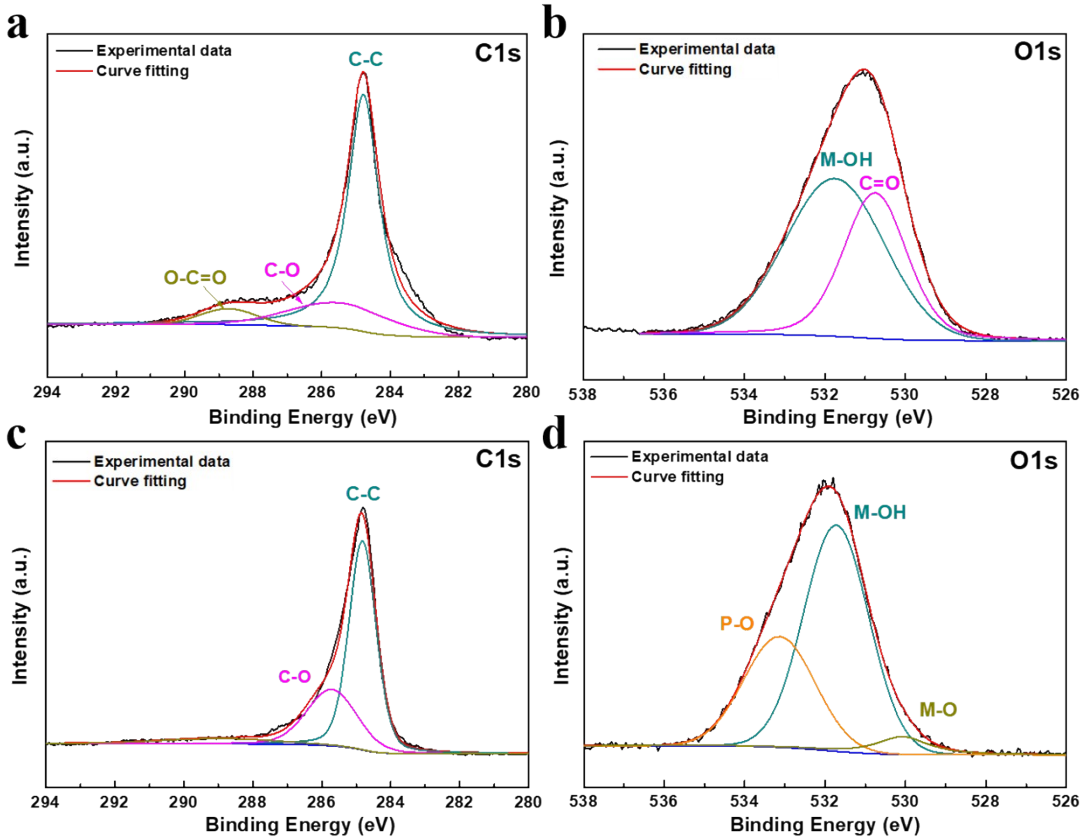

Fig. S8. High-resolution XPS spectra of C1s and O1s for (a, b) NiCo-ULAs, and (c, d) NiCoP@C-ULAs.

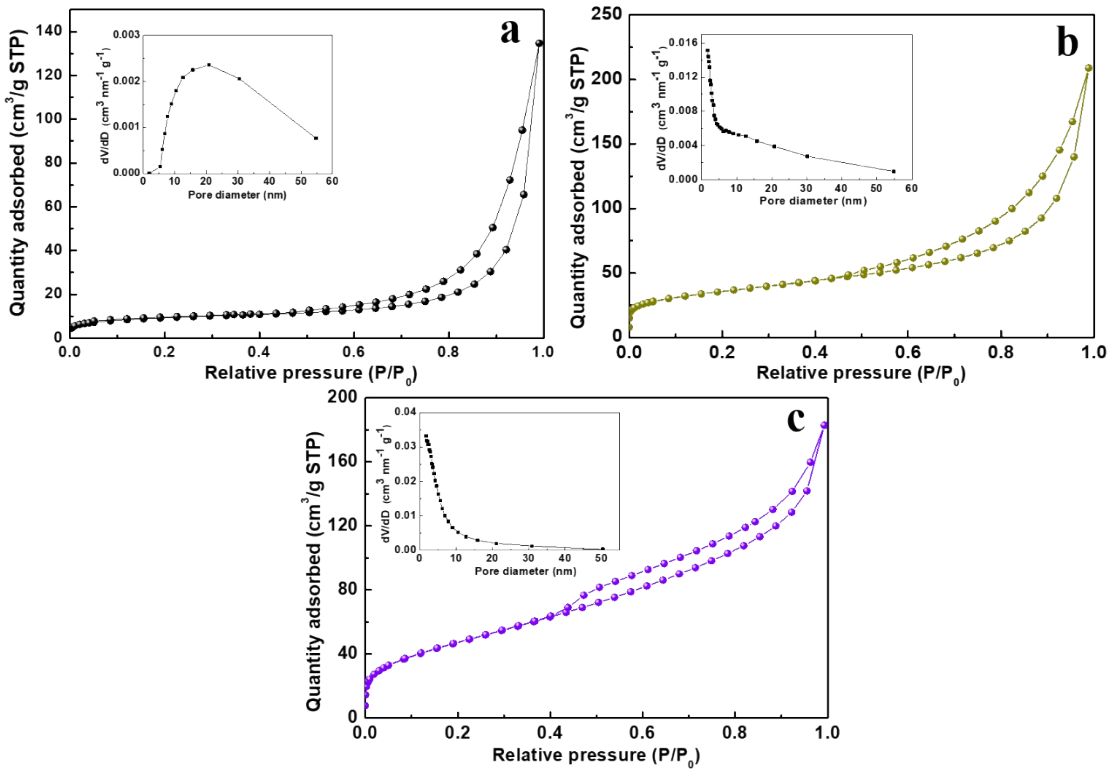

Fig. S9. Nitrogen adsorption–desorption isotherms of the (a) NiCo-NFAs, (b) NiCoP-NFAs, and (c) NiCoP@C-NFAs. Insets of (a) and (b), and (c) are their pore size distributions.

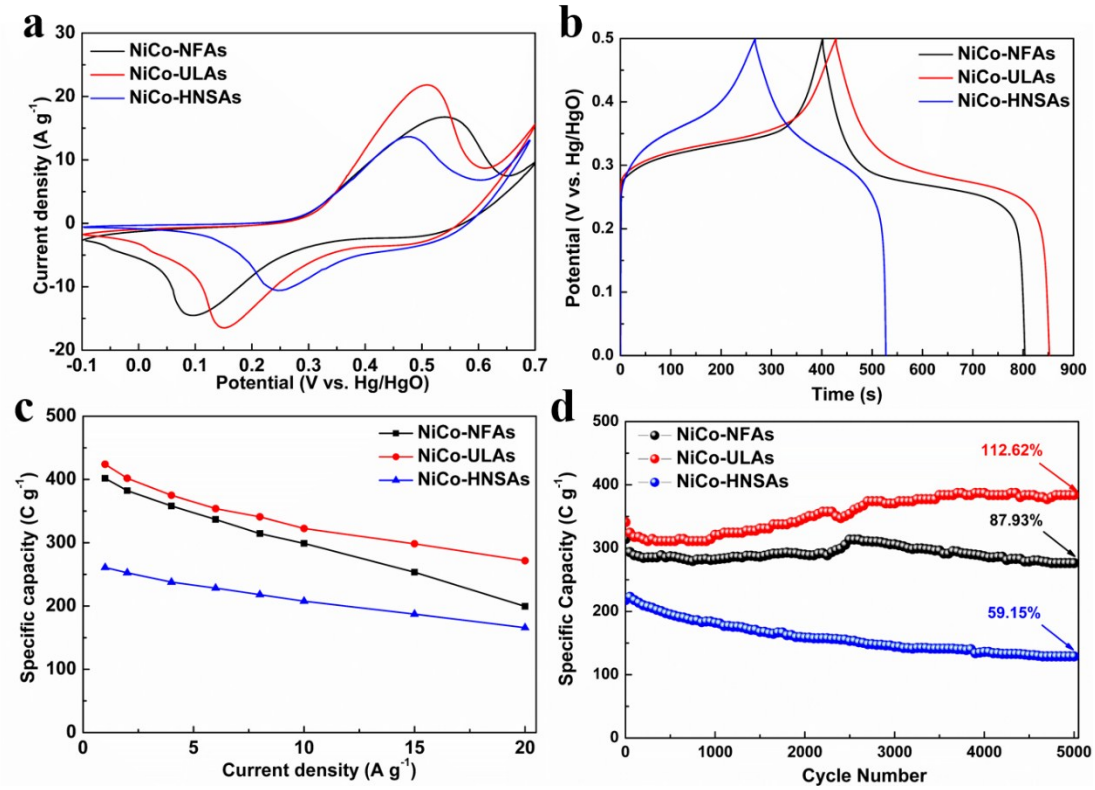

Fig. S10. Electrochemical performance of NiCo-NFAs, NiCo-ULAs, and NiCo-HNSAs precursors. (a) CV curves at a scan rate of 10 mV s^{-1}, (b) GCD curves at a current density of 1 A g^{-1}, (c) rate performance, and (d) cycling performance at a constant current density of 8 A g^{-1}.

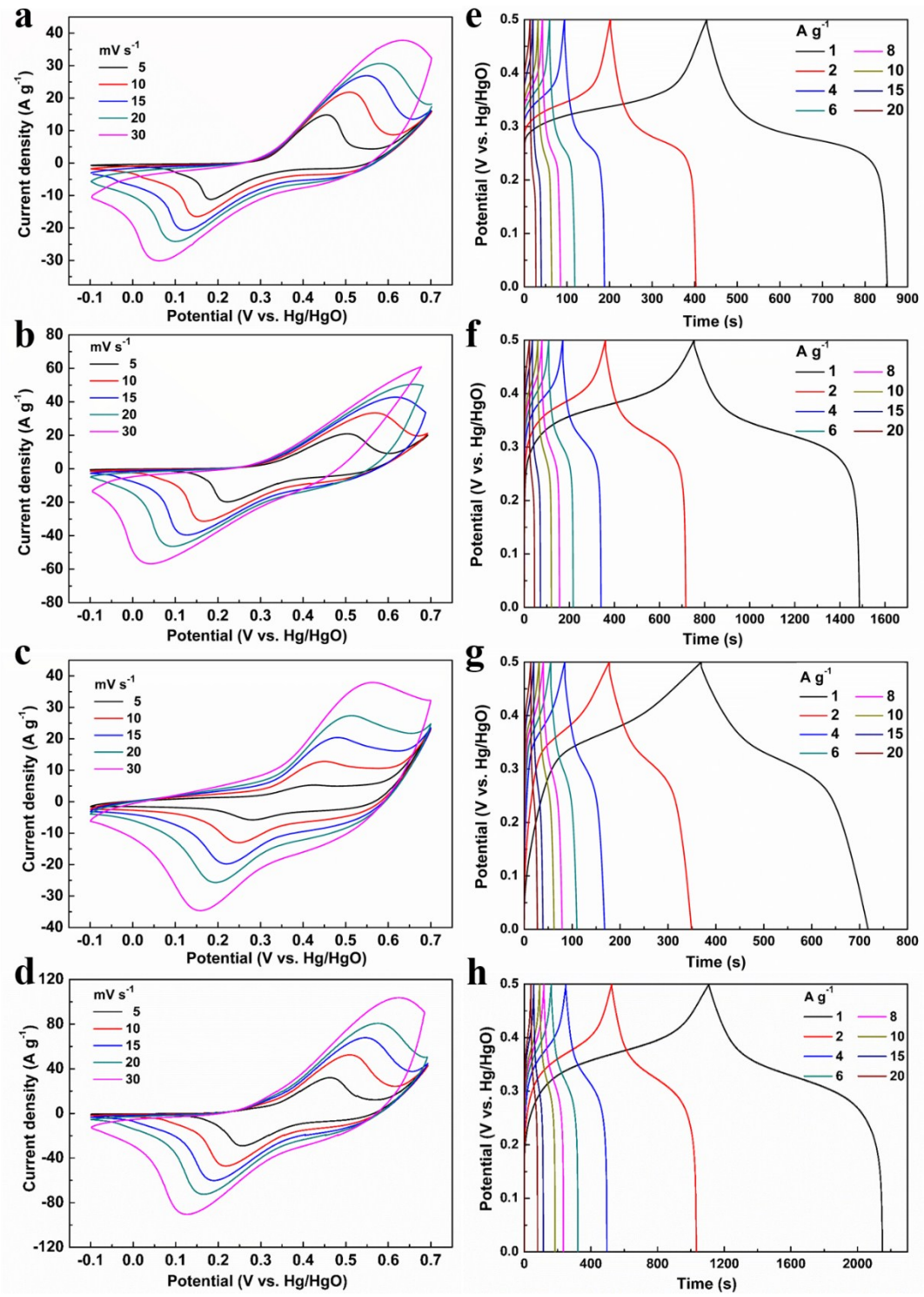

Fig. S11. (a-d) CV curves with different sweep rates, (e-h) GCD curves with different current densities of NiCo-ULAs, NiCoP-ULAs, $Ni_xCo_{1-x}O$@C-ULAs, and NiCoP@C-ULAs electrodes, respectively.

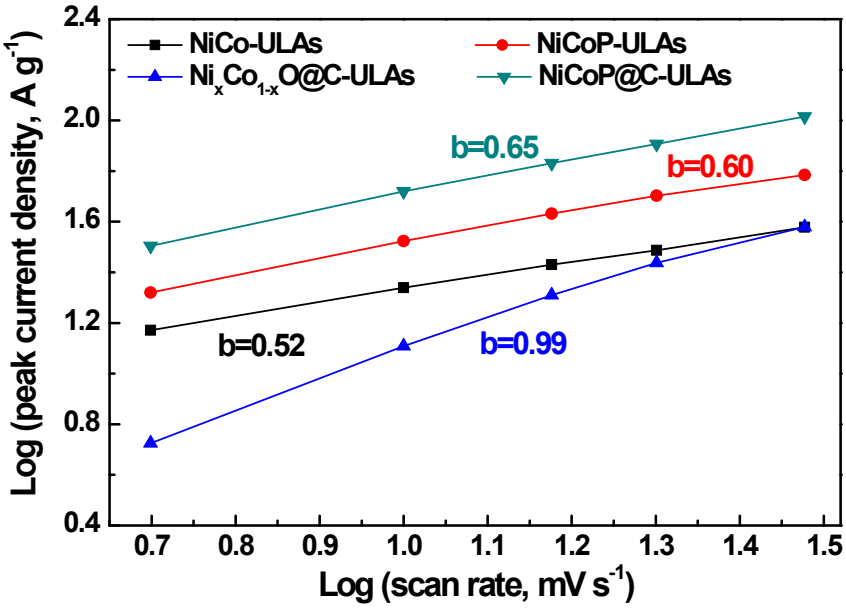

Fig. S12. Logarithm relationship between anodic peak current and scan rate for ULAs series electrodes.

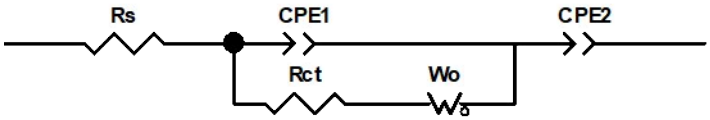

Fig. S13. The equivalent fitting circuit of ULAs series electrodes

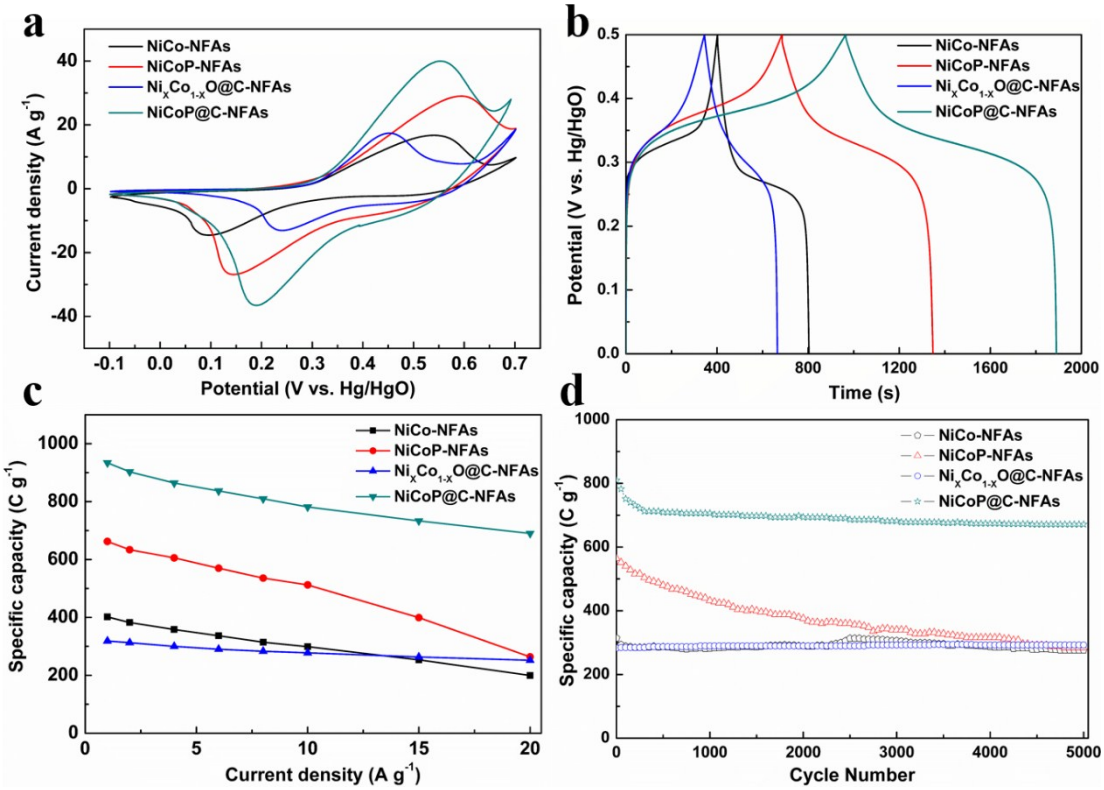

Fig. S14. Electrochemical performance of electrodes. (a) CV curves at a scan rate of 10 mV s^{-1}, (b) GCD curves at a current density of 1 A g^{-1}, (c) the specific capacity at different current densities, and (d) cycling performance at a constant current density of 8 A g^{-1}.

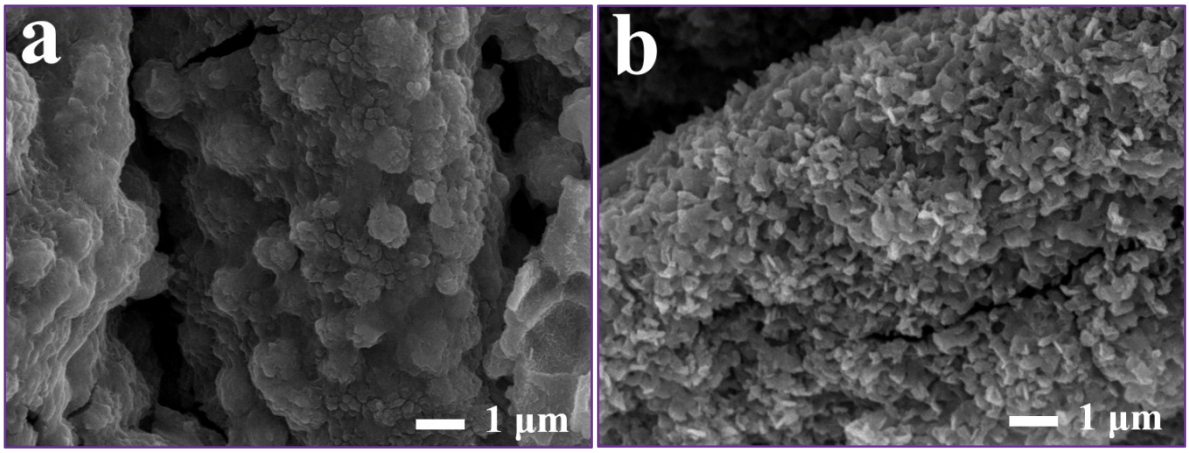

Fig. S15. SEM images of NiCoP-ULAs and NiCoP@C-ULAs after cycling for 5000 cycles.

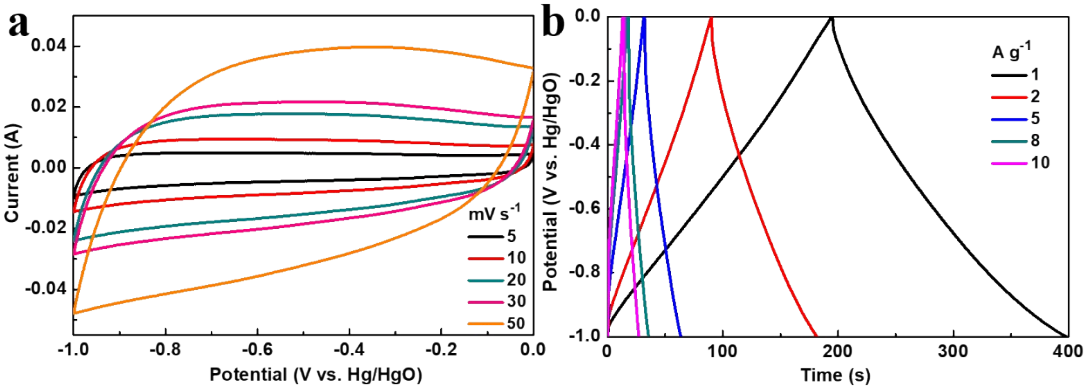

Fig. S16. Electrochemical performance of the AC electrode: (a) CV curves at different scan rates from 5 to 50 mV·s-1, (b) GCD curves at different current densities from 1 to 10 A·g^{-1}.

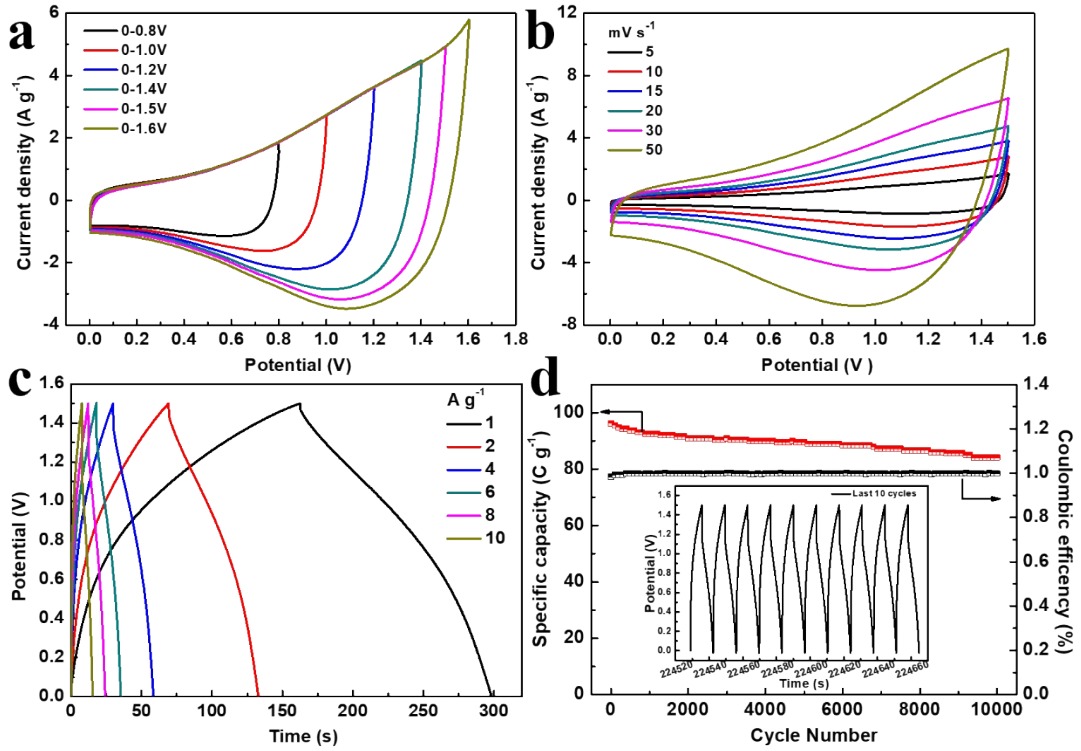

Fig. S17. (a) and (b) CV curves of the NiCoP@C-NFAs//AC ASC at different scan rates and voltage windows; (c) GCD curves of the NiCoP@C-NFAs//AC ASC at different current densities; (d) cycling performance of NiCoP@C-NFAs//AC at a current density of 8 A g^{-1}. The inset shows the last 10 cycles of the GCD curves of the ASC device.

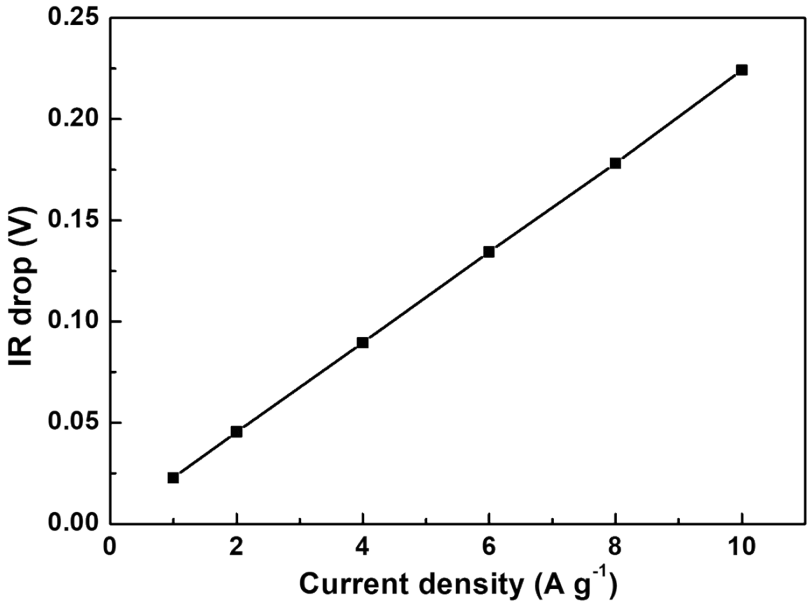

Fig. S18. The IR drop of the NiCoP@C-ULAs//AC device at different current densities.

Table S1. Textual parameters of the samples.

Sample	S_{BET} (m^2 g^{-1})	Average pore size (nm)	Total pore volume (cm^3 g^{-1})
NiCo-ULAs	37.5	16.8	0.181
NiCoP-ULAs	139.1	9.1	0.306
NiCoP@C-ULAs	201.9	4.4	0.231
NiCo-NFAs	31.4	21.3	0.209
NiCoP-NFAs	123.7	11.6	0.312
NiCoP@C-NFAs	174.4	6.1	0.293

Table S2. The electrochemical performances for as-prepared NFAs and ULAs series samples.

sample	Specific capacity (C/g)								Rate capability	Cycle stability (5000 cycles)
	1A/g	2A/g	4A/g	6A/g	8A/g	10A/g	15A/g	20A/g		
NiCo-NFAs	402	382	358	337	314	299	253	199	49.5%	87.9%
NiCoP-NFAs	662	634	606	570	536	512	399	264	39.9%	50.4%
$Ni_xCo_{1-x}O$ @C-NFAs	319	313	300	290	283	278	263	252	79.0%	103.4%
NiCoP@C-NFAs	934	903	864	837	810	782	733	690	73.9%	82.9%
NiCo-ULAs	424	402	375	354	341	322	298	272	64.2%	112.6%
NiCoP-ULAs	737	714	678	651	622	601	543	458	62.1%	55.1%
$Ni_xCo_{1-x}O$ @C-ULAs	349	343	333	323	315	310	292	273	78.2%	106.3%
NiCoP@C-ULAs	1046	1022	982	959	938	923	855	800	76.5%	86.3%

Table S3. Comparison of our ASCs devices performances with reported literatures

System	Device window (V)	Energy density (Wh kg^{-1})	Power density (W kg^{-1})	Cycle stability (cycles)	Ref.
AC//NiCoP	0-1.4	32	351	91.8% (3000)	1
NiCoP/NiCo-OH30//PC	0-1.6	34	775	92% (1000)	2
AC//CoP	0-1.4	19	350.8	96.7% (5000)	3
AC//NiP@$NiCo_2O_4$	0-1.4	21	350	78.3% (10 000)	4
NiCoP@NiCoP//AC	0-1.5	34.8	750	81.2% (10 000)	5
Ni_2P NS/NF//AC	0-1.4	26	337	91.3% (5000)	6
NiCoP//graphene	0-1.5	32.9	1301	83% (5000)	7
Ni_8Co_1P//AC	0-1.5	22.8	4320	No decay (5000)	8
sandwich-like LDH/rGO//rGO	0-1.6	34.5	772	86.7% (10 000)	9
Ni-P//AC	0-1.6	29.2	400	84.5% (1000)	10
Ni-Co-S//AC	0-1.5	21.6	134.9	90.0% (3000 cycles)	11
$NiCo_2O_4$//AC	0-1.5	27.4	493.2	79.2% (10 000)	12
NiCoP@C-NFAs//AC	**0-1.5**	**32.9**	**871.3**	**87.4% (10 000)**	**This work**
NiCoP@C-ULAs//AC	**0-1.5**	**37.1**	**792.8**	**91.4% (10 000)**	

References

1 Y.-M. Hu, M.-C. Liu, Y.-X. Hu, Q.-Q. Yang, L.-B. Kong and L. Kang, Electrochimica Acta, 2016, 215, 114-125.

2 X. Li, H. Wu, A. M. Elshahawy, L. Wang, S. J. Pennycook, C. Guan and J. Wang, Advanced Functional Materials, 2018, 28, 1800036.

3 Y. Hu, M. Liu, Q. Yang, L. Kong and L. Kang, Journal of Energy Chemistry, 2017, 26, 49-55. [4] Li X, Ding R, Yi L, Shi W, Xu Q, Liu E. Mesoporous Ni-P@$NiCo_2O_4$ composite materials for high performance aqueous asymmetric supercapacitors. Electrochimica Acta. 2016;222:1169-75.

4 X. Li, R. Ding, L. Yi, W. Shi, Q. Xu and E. Liu, Electrochimica Acta, 2016, 222, 1169-1175.

5 Y. Zhu, Q. Zong, Q. Zhang, H. Yang, Q. Wang and H. Wang, Electrochimica Acta, 2019, 299, 441-450.
6 K. Zhou, W. Zhou, L. Yang, J. Lu, S. Cheng, W. Mai, Z. Tang, L. Li and S. Chen, Advanced Functional Materials, 2015, 25, 7530-7538.
7 H. Liang, C. Xia, Q. Jiang, A. N. Gandi, U. Schwingenschlögl and H. N. Alshareef, Nano Energy, 2017, 35, 331-340.
8 R. Ding, X. Li, W. Shi, Q. Xu and E. Liu, Chemical Engineering Journal, 2017, 320, 376-388.
9 K. Le, Z. Wang, F. Wang, Q. Wang, Q. Shao, V. Murugadoss, S. Wu, W. Liu, J. Liu and Q. Gao, Dalton Transactions, 2019, 48.
10 D. Wang, L.-B. Kong, M.-C. Liu, W.-B. Zhang, Y.-C. Luo and L. Kang, Journal of Power Sources, 2015, 274, 1107-1113.
11 Y. Liu, Q. Lu, Z. Huang, S. Sun, B. Yu, U. Evariste, G. Jiang and J. Yao, Journal of Alloys and Compounds, 2018, 762, 301-311.
12 D. Zhao, H. Fang, A. Umar and W. Xiang, New Journal of Chemistry, 2018, 42.